

# Defects in antiferromagnetic nickel oxide

D. J. COATES, J. W. EVANS, K. H. WESTMACOTT

*Materials and Molecular Research Division, Lawrence Berkeley Laboratory, and  
Materials Science and Mineral Engineering, University of California, Berkeley,  
California 94720, USA*

Antiferromagnetic domain boundaries in single-crystal NiO specimens have been examined by transmission electron microscopy. The domain boundaries were found to move through the matrix as a result of beam-induced thermal stresses. Movement of the boundaries was restricted by dislocations. Some evidence is given to show that domain boundaries may serve as nucleation sites for the reduced species in gaseous reduction of NiO. The presence of vacancy loops in nickel oxide has been established.

## 1. Introduction

The reduction of nickel oxide to metallic nickel by means of gaseous reductants, particularly hydrogen, has been the subject of numerous investigations [1–6]. The techniques employed usually involve measuring macroscopic properties of the system, e.g. weight change, during the reduction experiment and then manipulating the data to produce a mathematical formulation of a general rate equation for the system (e.g. Szekeley and Evans [7, 8]). Whilst this type of investigation can be very successful, anomalies sometimes arise due to the fact that reduction processes occur on an atomic scale and possibly may be influenced by the presence of microscopic features such as grain boundaries or dislocations in the nickel oxide. In many reducing reactions there is a considerable induction period when no reaction, as measured macroscopically, occurs. This induction period is associated with the formation of nuclei of the reduced species which form only after the oxide has become sufficiently supersaturated with respect to the metal as oxygen is removed by the reducing gas. Nucleation of the reduction reaction occurs only at energetically favourable sites, so that the number of nuclei formed per unit surface area depends significantly on the condition of the surface.

Previous investigations have shown that the induction period for nickel oxide reduction is shortened by a factor of three to four and the rate of reaction is increased by a factor of two to three at 300 to 350°C when subjected to prior irradiation with 260 MeV protons [9]. An increased

reduction rate has also been observed with mechanically worked nickel oxide [10]. In both cases the effects were attributed to the crystal distortion produced by the radiation or plastic deformation processes resulting in higher energy sites in the crystal surface which facilitate the formation of nickel nuclei. Further evidence of the influence of the microstructure of the nickel oxide on its reduction behaviour is the well-documented observance of a change in activation energy of the reduction reaction at the Néel transformation temperature,  $T_N$  ( $\sim 250^\circ\text{C}$ ). Above this temperature nickel oxide is cubic and has the NaCl structure. Below this temperature NiO is antiferromagnetic and the magnetic spins of the nickel ions lying in adjacent (111) planes are oriented anti-parallel to one another. As a result of magnetostrictive interactions the lattice contracts slightly along a  $\langle 111 \rangle$  direction giving a rhombohedral structure. Different regions, or domains, in a given grain may contract along different  $\langle 111 \rangle$  directions. The boundaries between such domains are low-angle twin boundaries and lie along  $\{110\}$  and  $\{100\}$  planes. These domain walls have been observed in nickel oxide using neutron diffraction [11, 12], specular reflection [13] and electron microscopy [14–16], although only those domain boundaries lying on  $\{110\}$  planes have previously been imaged by electron microscopy. In order to observe the domains in transmission electron microscopy, two-beam dynamical conditions have to be used. From the resulting images certain features of the domains, such as direction of slope of the bound-

aries and contraction direction of the lattice can be deduced [15]. The observation that the density of nuclei also changes at the transformation temperature [5] suggests that the domain boundaries that intersect the surface of the specimens at temperatures below  $T_N$  may affect the distribution of energetically favourable nucleation sites.

The present work reports some features of the domain boundaries in nickel oxide, as well as some other crystal defects, as observed by transmission electron microscopy. Preliminary results of *in situ* reduction experiments on nickel oxide are also reported.

## 2. Experimental details

Specimens were obtained from single-crystal boules of nickel oxide by machining, abrading and ion-beam thinning to electron transparency. Further details of the specimens and preparation technique have been reported previously [17]. Specimens were examined on a 650 keV Hitachi microscope with double-tilt and heating stages. *In situ* reduction experiments were carried out in a Gatan environmental cell with a single-tilt platinum ribbon heating stage.

## 3. Results

Previously only one set of domain boundaries have been imaged on electron microscopy, due to the limitations of the crystallographic orientations of

the specimens used (the foils had (100) orientations so that {100}-type domain walls were not able to give fringe contrast). In the present work thin foils of nickel oxide were prepared with their surfaces approximately parallel to (111), (110) as well as (100) planes. Fig. 1 shows a number of domain boundaries imaged under two beam conditions in a (111) oriented foil. The domain boundaries intersect at various angles and hence must be both {100} and {110}-type boundaries. In some areas there appears to be some interaction between dislocations in the matrix and the domain boundaries, this is illustrated more graphically below. It is also apparent that the slightly different orientations of the lattice in adjacent domains gives rise to different contrast conditions so that the matrix appears alternately lighter or darker. The orientations of the domain boundaries can be analysed by trace analysis. Fig. 2 shows the results of such an analysis on two domain boundaries imaged under two-beam conditions ( $g = 220$ ). Fig. 2a is a bright-field micrograph and Fig. 2b a dark-field micrograph of the same area. The boundary labelled X is a (110)-type boundary, and that labelled Y is a (100)-type boundary.

The fringe patterns of the boundaries are due to dynamical coupling of the two-beams, which has been dealt with theoretically by Gevers *et al.* [15]. The nature of the edge fringes in each boundary under bright-field conditions is different, i.e. one is bright and one dark. Under dark-field imaging conditions the nature of the edge fringes in both domain boundaries is similar, both being bright in one boundary and dark in the other. According to the theoretical treatment and observations of Gevers *et al.* [15], the fringe corresponding to the intersection of the boundary with the upper surface is similar in nature in bright-field and dark-field images, whereas the lower edge fringe is "pseudo-complementary". The bottom and top edges of the domain boundaries in Fig. 2 are labelled "B" and "T", respectively. The boundaries thus both slope in the same direction.

Domain boundaries were observed to move readily through the foil due to the thermal stresses associated with the beam heating of the specimen. This is illustrated by the movement of the domain boundaries between the exposures of Fig. 2a and b with respect to the arrowed dislocation. Movement of the boundaries could be prevented by spreading the electron beam to dissipate the heating effect. Movement of the boundaries was also restricted by

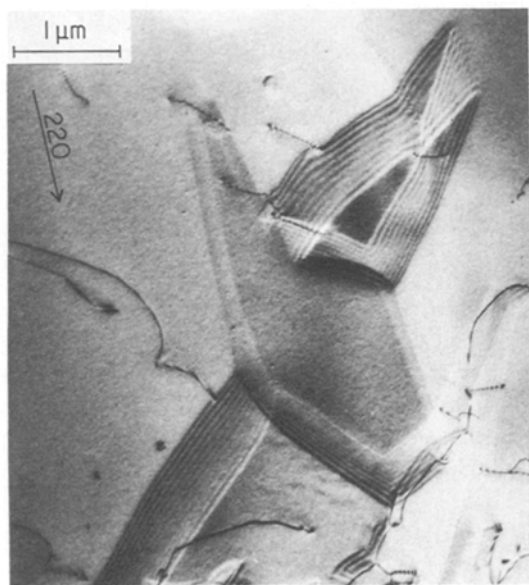


Figure 1 Antiferromagnetic domain boundaries in nickel oxide.

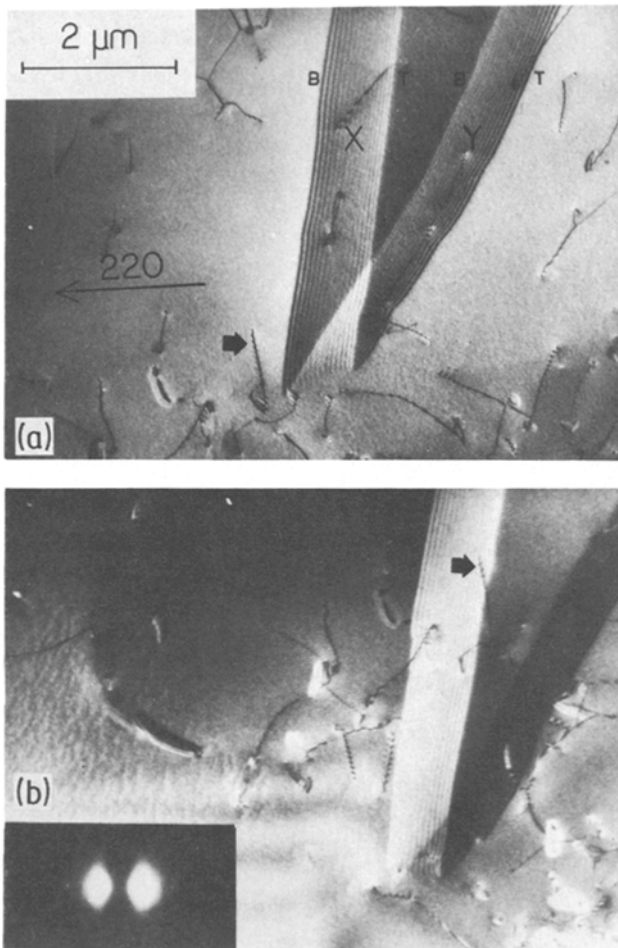


Figure 2 Bright-field and dark-field micrographs of domain boundaries: X, (110)-type boundary; Y, (100)-type boundary; B, bottom edge; T, top edge.

dislocation pinning. Figs. 3 and 4 show the effects of dislocations on the domain-boundary configuration. In some cases the pinned configuration was very stable and no amount of beam convergence induced movement of the domain boundaries. In an associated series of experiments, specimens were heated *in situ* and then cooled through the Neél temperature. In some areas domain boundaries were observed to reappear in approximately the same positions they were in before the heating cycle. These boundaries were generally the ones pinned by dislocations. Similar observations have been reported in antiferromagnetic MnO where dislocations generated by the formation of  $Mn_3O_4$  precipitates, as well as the precipitates themselves, were found to pin the domain boundaries [18].

Stable configurations of domain boundaries were also observed associated with low-angle grain boundaries within the nominally single-crystal material. Fig. 5 shows such a configuration. The planar defects toward the top of the micrograph

(labelled A) are low-angle grain boundaries and those toward the bottom (labelled B) are domain boundaries. Very little movement of these domain boundaries were found, even after extended periods of electron-beam impingement.

Fringe patterns were observed associated with some individual dislocations, as well as with the extended domain boundaries. The dislocation above the intersection of the domain boundaries in Fig. 2a shows such a feature. These were usually broader in extent at one end of the dislocation and grew thinner, sometimes disappearing, toward the centre of the dislocation. Fig. 6 shows a stereo pair of some dislocations with associated fringe patterns from which it is seen that the patterns are clearly associated with the dislocations. The fringe patterns disappeared when the specimens were heated above the Neél temperature, indicating that they are antiferromagnetic domain boundaries, so that it is apparent that some dislocations can stabilize small domains associated with them.

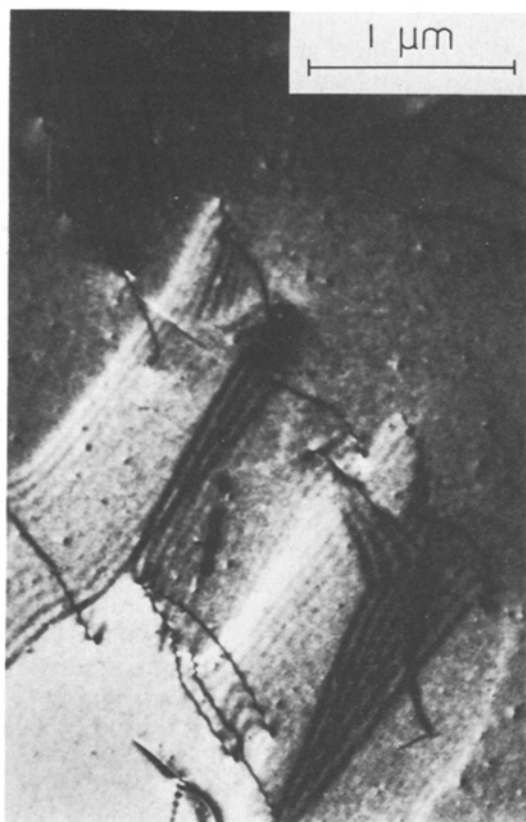


**Figure 3** Interaction of domain boundaries with dislocations.

Another feature of the nickel oxide structure which is apparent in a number of micrographs is the presence of dislocation loops (Figs. 5 and 6). Contrast experiments were conducted to determine the nature of the loops (see [19]), an example of which is shown in Fig. 7. In Fig. 7a the deviation parameter,  $s$ , has a positive value, as shown by the diffraction pattern, and the loop contrast lies outside the actual position of the loop. In Fig. 7b,  $s$  is negative and the loop contrast lies inside the loop position. From these observations, and the change in shape of the loop with further tilting, it is deduced that the loops are due to clusters of vacancies in the NiO lattice and are similar to those found in MgO [20, 21].

*In situ* reduction experiments have been carried out and some preliminary results are shown in Figs. 8 and 9. A nickel oxide specimen was heated in the environmental cell. The reducing temperature was about 220 to 250°C. A 10H<sub>2</sub>:90He gas mixture was used as the reductant at a pressure of 100 Torr. Fig. 8 shows an area after 13 and 31 min exposure and Fig. 9 shows the same area after 41

and 49 min exposure. Initially small nuclei of nickel developed and gradually covered the surface of the nickel oxide. After 13 min exposure (Fig. 8a) much of the NiO in the micrograph is covered with small nickel grains, with some areas apparently unaffected. With further reduction these areas also became covered with nickel grains. At a later stage many of the small nickel nuclei appeared unchanged, but in some areas “colonies” of nickel developed. Some of these colonies are arrowed in Fig. 8b and are aligned along a discrete band on the surface of the NiO, suggesting there may be some linear microstructural feature in the NiO influencing the formation of the colonies. After 41 min exposure (Fig. 9a) no change in the small nickel nuclei is observed, but the colonies have grown in size. Fig. 9b shows the area after 49 min exposure after which the specimen was cooled to room temperature. The specimen has been tilted to image any domain boundaries in the NiO substrate. Although the limitations of a single-tilt stage means it is difficult to obtain precise two-beam conditions in order to obtain good contrast conditions, some images of domain boundaries were obtained. One such boundary lies near the top of Fig. 9b, parallel to the row of colonies arrowed in Fig. 8b. Another domain boundary lies along the line of these colonies and may thus have influenced the formation of the colonies.

#### 4. Discussion and conclusions

The micrographs show clearly the presence of both {100} and {110}-type domain boundaries which were not imaged in previous TEM work [16]. It was found that thermal stresses can cause a redistribution of the domain walls although some configurations were stabilized by dislocation pinning. This could have a significant effect on the

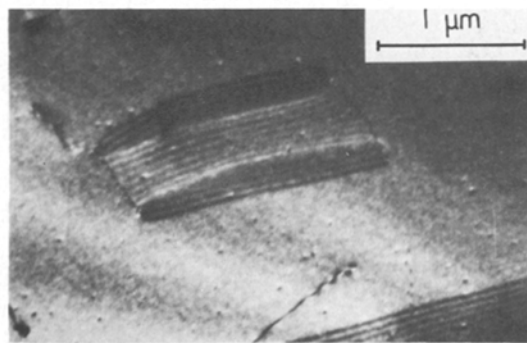


**Figure 4** Interaction of two domain boundaries with two dislocations, forming a small domain.

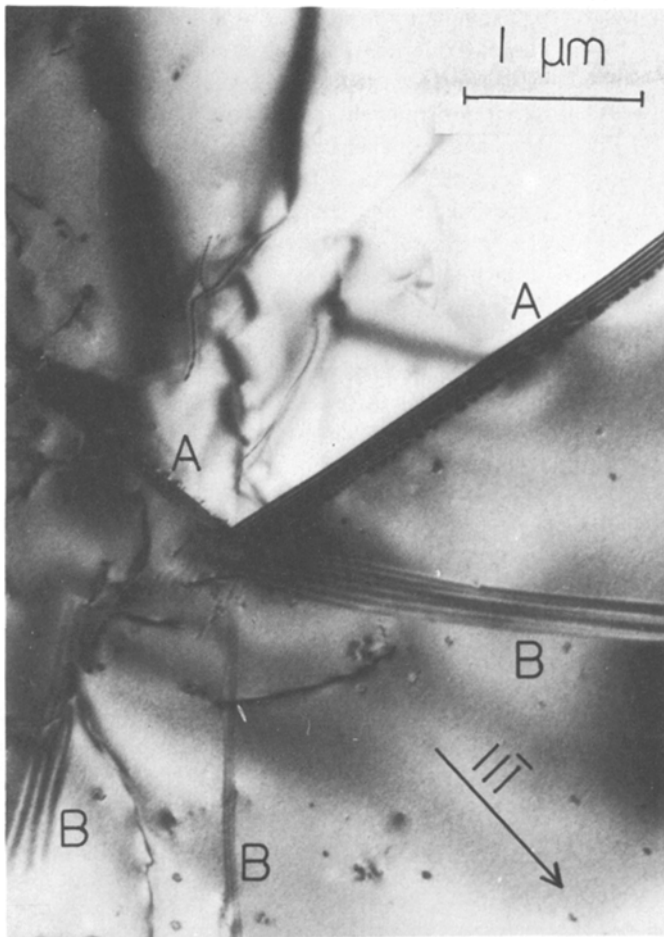


Figure 5 Bright-field micrograph of low-angle grain boundaries, A, and domain boundaries, B.

reduction of the nickel oxide at temperatures below  $T_N$  if, in fact, the nucleation process is influenced by the domain boundaries. Thus an increased number of dislocations in the original

nickel oxide resulting from prior working will cause pinning and retention of domain boundaries which might otherwise migrate to grain boundaries and be eliminated. Also individual dislocations

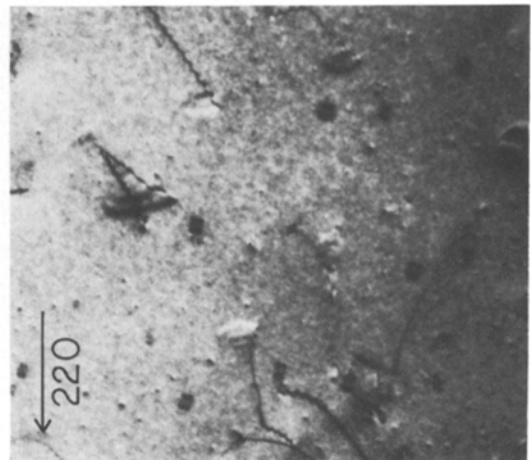
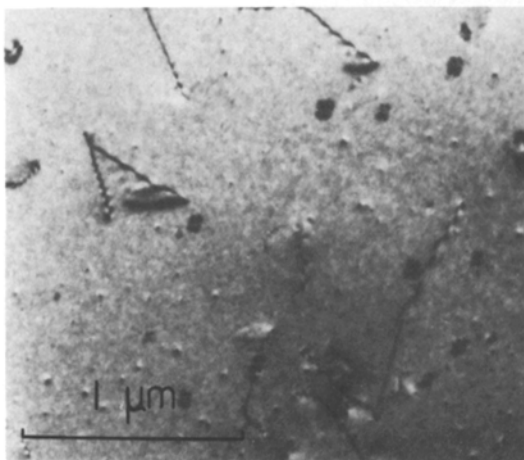


Figure 6 Stereographic pair (tilt  $\sim 10^\circ$ ) of dislocations and associated domain boundaries.

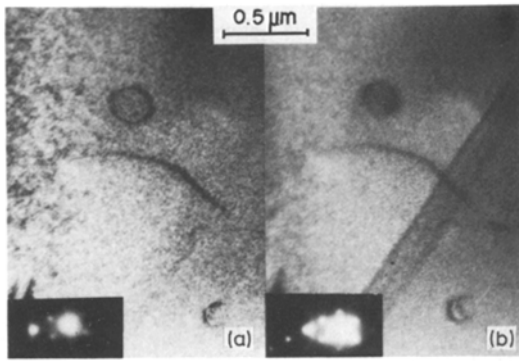


Figure 7 Dislocation loop in NiO, with  $s > 0$  and  $s < 0$ .

may have small domains associated with them. Thus previously worked nickel oxide will have a greater density of domain boundaries at reducing temperatures (below  $T_N$ ) than will fully annealed specimens.

Previous observations [17] indicate that dislocations themselves may have little influence on the nucleation sites of nickel on nickel oxide. The increased density of domain boundaries may provide an alternative explanation for the increase in reduction rates observed in mechanically worked specimens and presumed to be due to an increased density of nucleation sites.

Preliminary investigations into the reduction of nickel oxide indicate that domain boundaries may well influence the distribution of nickel "colonies" which are apparently a result of accelerated reduction of the nickel oxide in discrete regions. However, the evidence so far is not unequivocal. Further experiments are proceeding using an improved design furnace in the environmental cell, by which it is hoped to obtain unambiguous information concerning the role of domain boundaries in the nucleation of nickel.

The presence of vacancy loops in annealed nickel oxide, similar to those found in MgO [20, 21] has been established. In MgO the loops appeared in rows and were attributed to having originated as elongated dislocation dipoles. Rows of dislocation loops have also been observed in the wake of dislocations in NiO [16] suggesting a similar mode of formation, although in the present study the loops appear individually dispersed and not associated with dislocations.

#### Acknowledgement

This work was supported by the Division of Materials Sciences, Office of Basic Energy Sciences, US Department of Energy under contract no. W-7405-Eng-48.

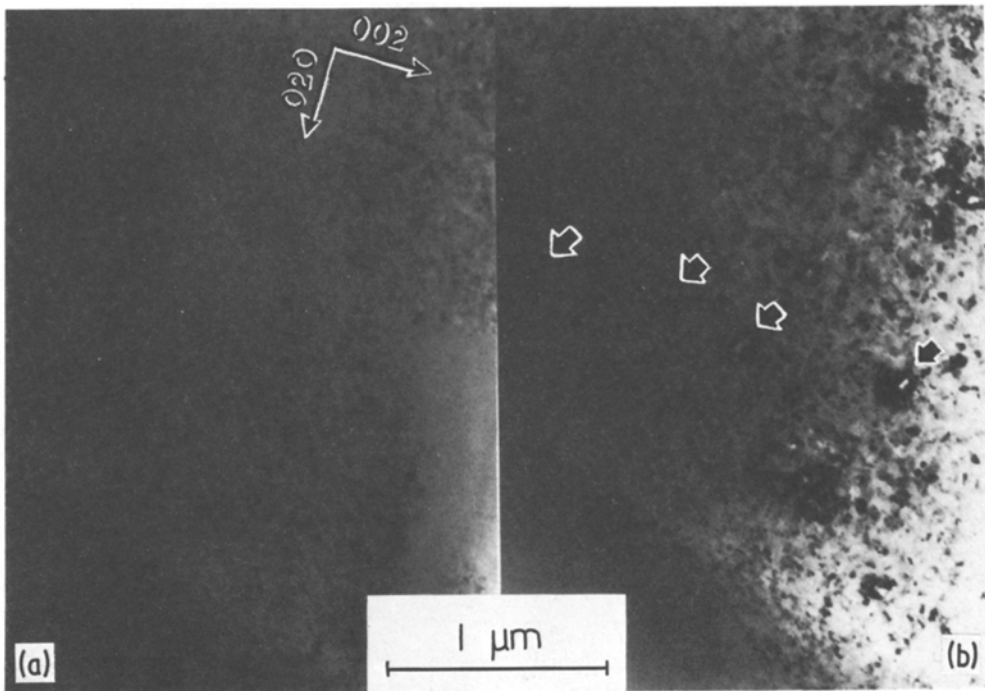


Figure 8 *In situ* reduction of NiO in  $10\text{H}_2:90\text{He}$  after 13 and 31 min reduction ( $T \sim 220$  to  $250^\circ\text{C}$ ).

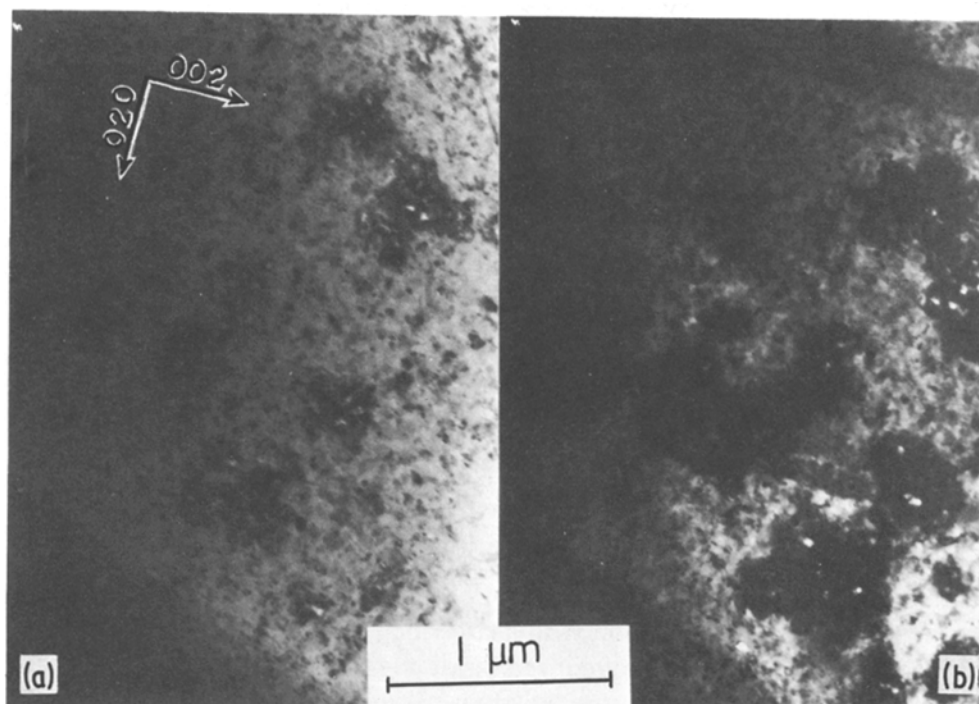


Figure 9 In situ reduction of NiO in 10H<sub>2</sub>:90He after 41 and 49 min reduction ( $T \sim 220$  to  $250^\circ\text{C}$ ).

## References

1. G. PARRAVANO, *J. Amer. Chem. Soc.* **74** (1952) 1194.
2. J. SZEKELY, C. I. LIN and H. Y. SOHN, *Chem. Eng. Sci.* **28** (1973) 1975.
3. J. W. EVANS, PhD Dissertation, State University of New York at Buffalo (1970).
4. F. CHIESA and M. RIGAUD, *Can. J. Chem. Eng.* **49** (1971) 617.
5. A. ROMAN and B. DELMON, *Compt. Rend. Ser. B* **269** (1969) 801.
6. *Idem, ibid.* **271** (1970) 77.
7. J. SZEKELY and J. W. EVANS, *Met. Trans.* **2** (1971) 1691.
8. *Idem, ibid.* **2** (1971) 1699.
9. M. T. SIMNAD, R. SMOLUCHOWSKI and A. SPILNERS, *J. Appl. Phys.* **29** (1958) 1930.
10. Y. IIDA and K. SHIMADA, *Bull. Chem. Soc. Jap.* **33** (1964) 1194.
11. J. C. MARMEGGI and J. BARUCHEL, *J. Mag. Mag. Mats.* **10** (1979) 14.
12. W. L. ROTH, *J. Appl. Phys.* **31** (1960) 2000.
13. G. A. SLACK, *ibid.* **31** (1960) 1571.
14. P. DELAVIGNETTE and S. AMELINCKX, *Appl. Phys. Lett.* **2** (1963) 236.
15. R. GEVERS, P. DELAVIGNETTE, H. BLANK and S. AMELINCKX, *Phys. Stat. Sol.* **4** (1964) 383.
16. R. GEVERS, P. DELAVIGNETTE, H. BLANK, J. VAN LANDUYT and S. AMELINCKX, *ibid.* **5** (1964) 595.
17. J. LITTLE, J. W. EVANS and K. WESTMACOTT, *Met. Trans.* **11B** (1980) 519.
18. D. J. BARGER and R. G. EVANS, *J. Mater. Sci.* **6** (1971) 1237.
19. G. THOMAS and M. J. GORINGE, "Transmission Electron Microscopy" (Wiley, New York, 1979).
20. G. W. GROVES and A. KELLY, *Phil. Mag.* **6** (1961) 1527.
21. *Idem, ibid.* **7** (1962) 892.

Received 26 February  
and accepted 23 April 1982